2006-06-07

Mechanisms of the Wurtzite to Rock Salt Phase Transitions in Galium Nitride

Jesse Z. Gunter
Brigham Young University - Provo

MECHANISMS OF THE WURTZITE TO ROCK SALT PHASE TRANSITIONS IN GALIUM NITRIDE

by

Jesse Z. Gunter

A thesis submitted to the faculty of

Brigham Young University

in partial fulfillment of the requirements for the degree of

Master of Science

Department of Physics and Astronomy

Brigham Young University

August 2006

BRIGHAM YOUNG UNIVERSITY

GRADUATE COMMITTEE APPROVAL

of a thesis submitted by

Jesse Z. Gunter

This thesis has been read by each member of the following graduate committee and by majority vote has been found to be satisfactory.

Date	Harold T. Stokes, Chair
Date	Dorian M. Hatch
Date	James P. Lewis

BRIGHAM YOUNG UNIVERSITY

As chair of the candidate's graduate committee, I have read the thesis of Jesse Z. Gunter in its final form and have found that (1) its format, citations, and bibliographical style are consistent and acceptable and fulfill university and department style requirements; (2) its illustrative materials including figures, tables, and charts are in place; and (3) the final manuscript is satisfactory to the graduate committee and is ready for submission to the university library.

_____ _____

Date

Harold T. Stokes
Chair, Graduate Committee

Accepted for the Department

_____

Ross L. Spencer
Graduate Coordinator
Department of Physics and Astronomy

Accepted for the College

_____

Thomas W. Sederberg
Associate Dean
College of Physical and Mathematical Sciences

ABSTRACT

MECHANISMS OF THE WURTZITE TO ROCK SALT

PHASE TRANSITIONS IN GALIUM NITRIDE

Jesse Z. Gunter

Department of Physics and Astronomy

Master of Science

We studied the wurtzite to rock salt phase transition in gallium nitride (GaN). Using the mapping algorithm of COMSUBS we found 435 possible mechanisms for this transition. We then used FIREBALL to do density functional theory calculations and found enthalpy barrier heights for the transition pathway. We used this to determine the mechanisms that are the most favorable for GaN. The most favorable mechanisms for GaN are those that break no bonds during the phase transition. The bond-preserving mechanisms involve bilayer sliding of (010) hexagonal plane in the plus or minus [100] hexagonal direction.

ACKNOWLEDGMENTS

The author wishes to acknowledge Dr. Harold Stokes whose unfailing support is greatly appreciated. He thanks Dr. James P. Lewis and his group for the use of the computer lab and their help with FIREBALL. He thanks Dr. Dorian Hatch, J.J. Dong of Auburn University and the others who collaborated on this project for their valuable help and insights. Funding thanks to DOE – BSE. Thanks also to the Department of Physics and Astronomy at Brigham Young University for all of its support.

TABLE OF CONTENTS

LIST OF FIGURES

I Introduction and Background

Gallium nitride (GaN) is a type III-V semiconductor widely used in science and industry. As the uses for GaN become more sophisticated, a more in-depth knowledge is needed of its properties under conditions that are more and more extreme. Studying phase transitions of GaN will help us to theoretically understand and in some cases even theoretically predict these properties. GaN is most commonly found in the wurtzite crystalline structure. The atoms in the wurtzite structure of GaN rearrange into the rock salt structure when put under extreme high pressure. This phase transition is the one that we investigated for GaN.

The wurtzite structure is hexagonal and for GaN contains equal amounts of gallium and nitrogen. Wurtzite has the symmetry of $P6_3mc$ (space group 186) with both N and Ga at Wyckoff position b but with different z values (see appendix A). Wurtzite's conventional unit cell, shown in Figure 1, contains four atoms. This is the smallest possible unit cell size for wurtzite. The lattice parameters *a* and *b* are the length of the sides as shown, while the lattice parameter *c* is the height of the unit cell. Each circle represents two atoms in the unit cell, one of each kind. At the positions of the black circles there is a nitrogen atom at z = 0 and a gallium atom at z = u, where u is about but not exactly 3/8 of *c*. At the white positions there is a nitrogen atom at z = 0.5*c* and a gallium atom at z = 0.5*c* + u (approx. 7/8*c*). This unit cell, as do all unit cells in a crystal, stacks and repeats in the directions of the lattice vectors **a**, **b**, and **c**.

The rock salt structure is face centered cubic and for GaN also contains equal amounts gallium and nitrogen. Rock salt has the symmetry of Fm-3m (space group 225) with N

and Ga at Wyckoff positions a and b respectively (see Appendix A). The conventional unit cell (thin line) is the larger of the two unit cells in Figure 2. This unit cell contains eight atoms. The smaller unit cell is marked (thick line) because it is the most easy to compare with the wurtzite structure. At the positions of the black circles there is a nitrogen atom at z = 0 and a gallium atom at z = 0.5*c*. At the white positions there is a nitrogen atom at z = 0.5*c* and a gallium atom at z = 0 (can be thought of as z = 1.0*c* when comparing to the wurtzite structure). The smallest unit cell possible for the rock salt structure contains only two atoms, but it is not important for this case because it is smaller than the wurtzite's smallest unit cell.

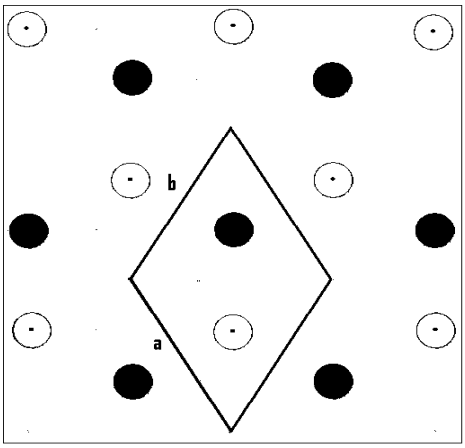

Figure 1. Wurtzite conventional unit cell containing 4 atoms, 2 for each circle

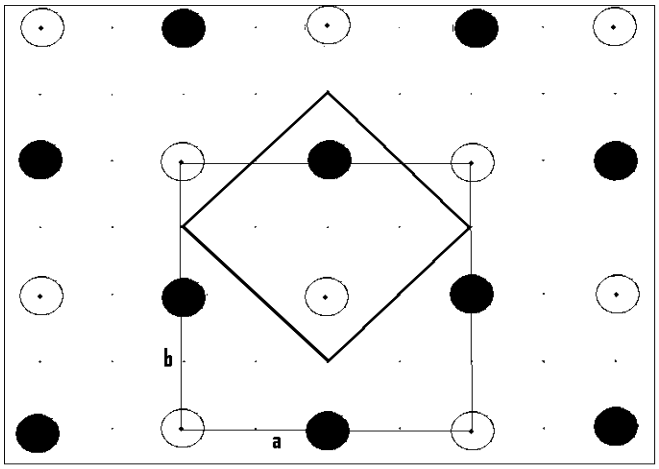

Figure 2. Rock salt conventional unit cell (thin line) with 8 atoms and smaller unit cell chosen with 4 atoms like the wurtzite conventional unit cell (thick line)

There are a number of ways to theoretically study the paths that atoms follow when a crystal undergoes a phase transition from one structure to another. One option is to make a physical model of the two structures and then try to visually see possible paths that the

atoms could follow. A second option is to run molecular dynamics simulations and try to force the atoms to go from the crystal's original structure to the final structure. Finally you can use mapping algorithms to chart possible atomic paths. We used this last approach in the study of this phase transition.

My research on GaN is a continuation of our previous work on SiC. I used the same methods and procedures for GaN that we used for SiC (Hatch 2005). I helped further develop and refine the computational methods for identifying and optimizing favorable mechanisms. I applied these methods to find and optimize mechanisms for GaN in the wurtzite to rock salt phase transition. From the most favorable mechanisms found I reasoned out qualitatively how the atoms move during the phase transition and obtained a general mechanism.

II Methods and Procedures

The first thing we had to do was optimize the structural parameters of the wurtzite and rock salt structures of GaN for their lowest enthalpy. We used FIREBALL (Lewis 2001), which uses density functional theory and pseudopotentials, to do our electronic and energy calculations. For each structure we started with the structural parameters found in the literature and adjusted them one by one until we found the structural parameters that gave us the lowest enthalpy.

For the wurtzite structure of GaN, at zero pressure and 0 K, we obtained the following optimized structure for the conventional unit cell:

$a = b = 3.38$Å, $c = 5.58$Å

N at	0.333333	0.666667	0.000000
	-0.333333	0.333333	0.500000
Ga at	0.333333	0.666667	0.375
	-0.333333	0.333333	0.875

All the atomic positions are fractions of the conventional unit cell's lattice vectors (**a**, **b** or **c**). The adjustable parameters for the wurtzite structure are length of the lattice parameters *a* and *c* and the z position of one of the gallium atoms. The symmetries of wurtzite require that *a* and *b* be of equal length and the z positions of the gallium atoms be ½ *c* apart. The x and y atomic positions of GaN and the z positions of the nitrogen atoms are also fixed by the space group symmetry. The angle between the lattice vectors **a** and **b** is 120 degrees. The other two angles between the lattice vectors are both 90 degrees.

The measured values for the lattice parameters of GaN's wurtzite structure are

$a = b = 3.19$Å, $c = 5.19$Å (H. Xia 2003). Our calculated values for a is 6.0 percent larger than the experimental value and our value for c is 7.5 percent larger. The value of c/a is only 1.5 percent larger than the experimental value. This means that qualitatively our structure has the right shape, but the overall volume is just a little off. To get better values than this, either something different needs to be done to improve the accuracy of FIREBALL for GaN, which was not my part of the project, or we need to use a different program that is more accurate, but uses a whole lot more computing time. Too much computing time is a problem because of how many times we have to recalculate similar structures along the transition pathway while doing the optimization of the structural parameters for each mechanism.

For the rock salt structure of GaN, at zero pressure and 0 K, we obtained the following optimized structure for the conventional unit cell:

$a = b = c = 4.50$Å

N at	0.000000	0.000000	0.000000
	0.000000	0.500000	0.500000
	0.500000	0.500000	0.000000
	0.500000	0.000000	0.500000
Ga at	0.000000	0.500000	0.000000
	0.000000	0.000000	0.500000
	0.500000	0.000000	0.000000
	0.500000	0.500000	0.500000

The only parameter that we allow to change, because of the symmetry of the rock salt structure, is the length of the unit vectors which are all required to be equal. There are no experimental values for the rock salt structure of GaN at zero pressure because it is only stable under high pressures.

We next found the pressure at which the two structures have equal enthalpies after being reoptimized at that pressure. At zero pressure the wurtzite structure has a lower enthalpy than the rock salt structure, -20.3 eV per atom compared with -19.8 eV per atom (using our FIREBALL calculations). As the pressure is increased the difference in the enthalpies decrease. At 60 GPa the enthalpies are equal at -16.0 eV per atom. This pressure is used as the theoretical prediction of the pressure at which the phase transition takes place.

The phase transition pressure we obtained for GaN is higher the then highest theoretical value we found in the literature. Most theoretical values sited by Limpijumnong (2001) are in the 51 to 55 GPa range. Limpijumnong's calculations gave him a value of 31 GPa. Our value is also higher than the highest experimental value. Experimental values for the phase transition pressure vary widely from about 37 to 52 GPa (Limpijumnong 2001). The wide range of experimental values seem to stem from difficulty of the experiments and the large differences in the methods used to cause and measure the phase transition.

The reason our value is above both the experimental and theoretical ranges is because FIREBALL did not work as well for GaN as for the other materials we have used FIREBALL for. Our phase transition pressure being higher then we expected is consistent with our unit cells being too large.

We inputted the structural parameters of the structures that have equal enthalpy into COMSUBS. COMSUBS is a program developed by Stokes and Hatch (2004) that uses a mapping algorithm to map one crystalline structure onto another; this is done using

different orientations and unit cell sizes. New unit cells are chosen in both structures and a pathway is extrapolated between them. The chosen unit cells both have the same number of atoms for each structure and each unit cell contains a number of atoms that is a whole number multiple of the number in the smallest unit cell of that crystal, also known as a primitive unit cell. In the case of GaN, the wurtzite primitive unit cell contains four atoms and the rock salt primitive unit cell contains two atoms, so the number of atoms in the new unit cells must be a multiple of four.

After finding the possible mappings between the two structures, COMSUBS sorts through the possible pathways and gives as output the ones that meet the constraints that were given in the input file. Among the possible constraints are maximum and minimum cell size, atomic displacement, maximum strain and the minimum distance between atoms along the path. COMSUBS gives the structural parameters of each mechanism in terms of a subgroup that holds for the whole pathway. The symmetries of the common subgroup are a product of the relative orientations and cell sizes chosen for the mapping.

The following is the input file we used for our main run of COMSUBS:

```
GaN
186   ! space group symmetry of crystal 1 (Wurtzite)
3.08 3.08 5.06 90 90 120   ! lattice parameters: a,b,c,alpha,beta,gamma
2   ! number of Wyckoff positions
N 0.3333333333   0.666666667   0.00000
Ga  0.333333333   0.666666667   0.37400
225   ! space group symmetry of crystal 2 (rock salt)
4.19 4.19 4.19 90 90 90   ! lattice parameters: a,b,c,alpha,beta,gamma
2   ! number of Wyckoff positions
N 0 0 0
Ga 0.5 0.5 0.5
size 1 2   ! limit subgroup to cell doubling
strain 0.6 1.6   ! minimum and maximum strain allowed
neighbor 1.5   ! minimum nearest-neighbor distance between atoms along path
```

```
shuffle 2   ! maximum atomic displacement
fireball
N 7
Ga 31
```

The first line is the title of the file. Anything after an exclamation mark is a comment. Notice we have not listed all the atomic positions that we did earlier. COMSUBS calculates the position of the other atoms based on the given space group symmetry. Appendix A contains some of the space group information that is used by COMSUBS. We adjusted the constraints in the input file until COMSUBS gave us 435 mechanisms for the wurtzite to rock salt phase transition. We limited the run to a maximum cell size of 8 atoms, which corresponds to two wurtzite primitive unit cells or four rock salt primitive unit cells. The last three lines of the input file are the command for COMSUBS to use FIREBALL to calculate an estimate of the barrier height of each transition mechanism.

COMSUBS finds an estimate of the barrier height by looking for the highest enthalpy along the pathway while changing the structural parameters linearly from the initial to the final structure. The difference between the enthalpy at the end points and the highest enthalpy is used as an estimate of the barrier height of the transition. The amount of energy needed to overcome the barrier determines the speed of the transition at different temperatures and how stable the higher pressure structure is at lower pressures. Figure 3 is a histogram of the mechanisms that have an estimated barrier height of less than 1 eV per atom. The barrier height estimate from the linear pathway is always an overestimate of the barrier height for that mechanism.

We found the true barrier height for each mechanism we studied by using bow functions (Hatch 2005). Bow functions allow each independent variable to change on a different quadratic curve while changing the crystal from the initial to final structure, instead of in lockstep as was done for the linear path. This allows the different structural parameters to change at different relative rates at different points along the pathway. At the half way point, instead of all parameters being half changed some can be barely changed while others can be mostly changed.

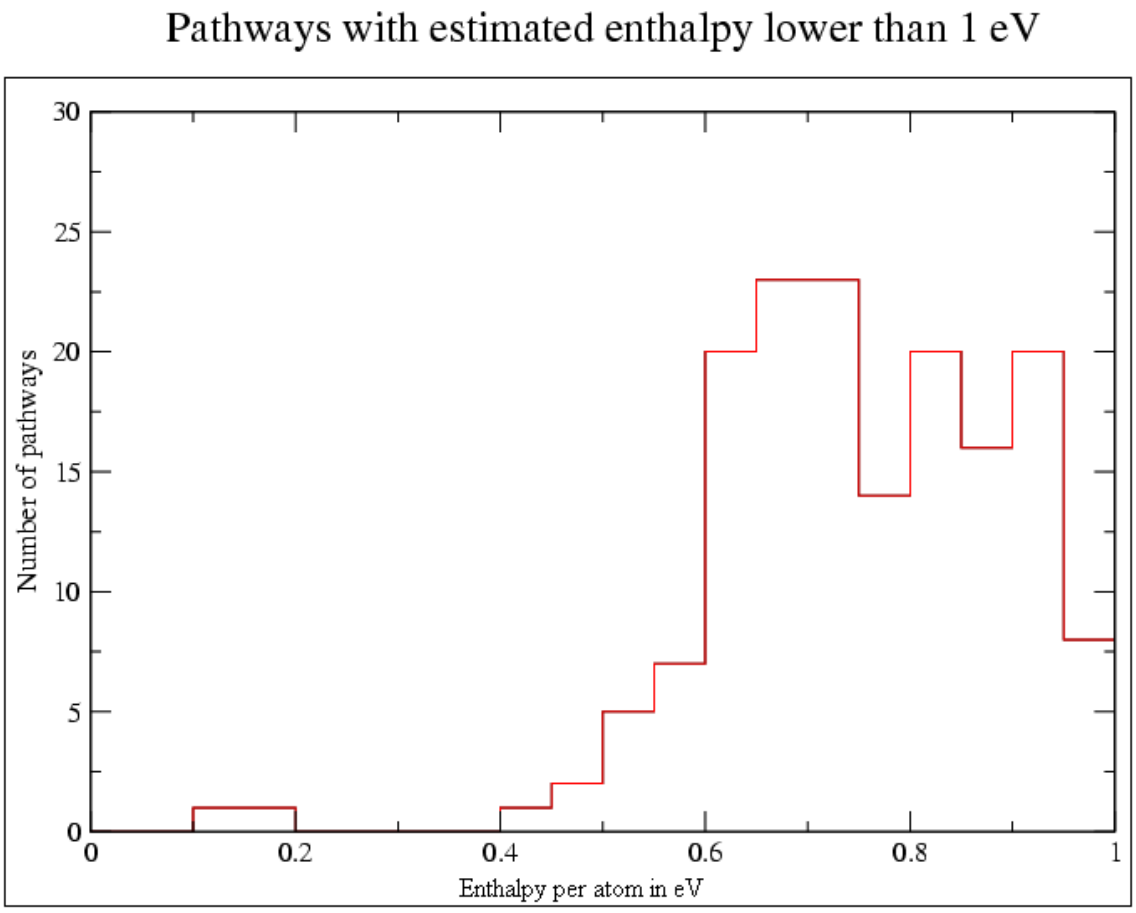

Figure 3. Histogram of mechanisms with estimated barrier height of less than 1 eV

When we used bow functions for silicon carbide, the mechanisms with the lowest

barrier height using the linear pathway estimate still had the lowest barrier height after relaxation with bow functions. Knowing this helps us to focus our efforts on the most promising mechanisms.

As can be seen from the histogram, two of the mechanisms have a much smaller barrier height for the linear path than the others. The mechanism with the larger energy of the two, listed as Subgroup 1 in appendix B, has only 4 atoms in the unit cell and has the symmetry of $Cmc2_1$ (space group 36). This is the path that we most commonly found in the literature and we found it in three different sources. A research paper by H. Sowa (2001) proposed a mechanism that follows the symmetry of *Cmcm* (space group 8), but a visual comparison shows it is the same basic mechanism and is just a lower symmetry version of our path. Limpijumnong and Lambrecht (2001) explain the structure of the transition mechanism mostly graphically, and they give little information about the symmetries that hold during the transition except it is orthorhombic, but a careful examination shows it is the same mechanism. This mechanism was also one of three paths found by Shimojo (2004), labeled as RS-I, using molecular dynamic simulations for the wurtzite to rock salt transition in CdSe.

Figure 4 is the wurtzite structure of this transition mechanism and shows how the atoms move in plane pairs. The gallium atoms move a little up (in the *c* direction) *so* they all have the same z coordinate as the nitrogen atoms and a little to the side so that the spacing between the moving planes all become equal. The main movement of the atoms are in the [100] direction. The (010) planes of the wurtzite structure then become the (110) planes of the rock salt structure. As can be seen from Figures 4 and 5, each pair of planes move about one half of the lattice vector length *a* verses the pair before it.

Another way to look at it is each unit cell, if chosen like the unit cell in Figure 1, is squished into the smaller of the two unit cells shown in Figure 2 with the same deformation happening in the crystal as a whole. This mechanism, though fairly favorable on the local scale, requires a large strain and deformation in the crystal as a whole.

The mechanism with the lowest barrier height on the histogram, listed as Subgroup 2 in appendix B, is for a mechanism that involves a cell size of 8 atoms and has the symmetry of $Pna2_1$ (space group 33). Shimojo also had this one in his paper labeled as RS-II. The thing that both of these mechanisms have in common is that neither one of them involve breaking any bonds for the wurtzite to rock salt phase transition.

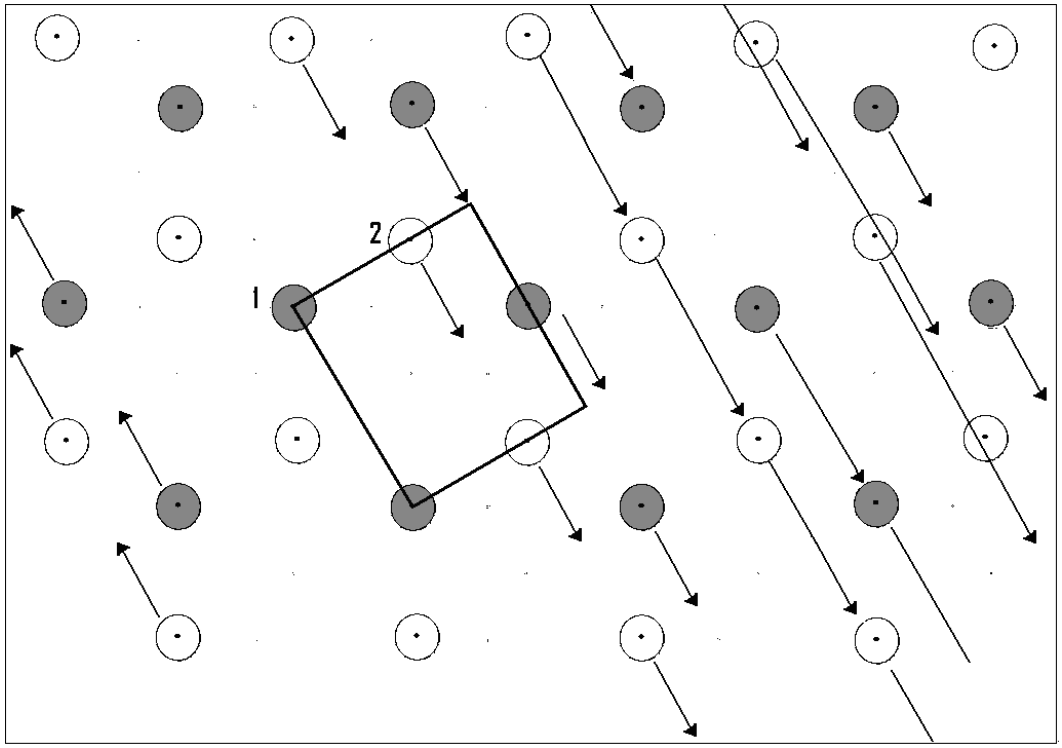

Figure 4. Transition mechanism with 4 atoms, 2 atom pairs, in the unit cell. Each pair of planes slides the same amount relative to the pair before.

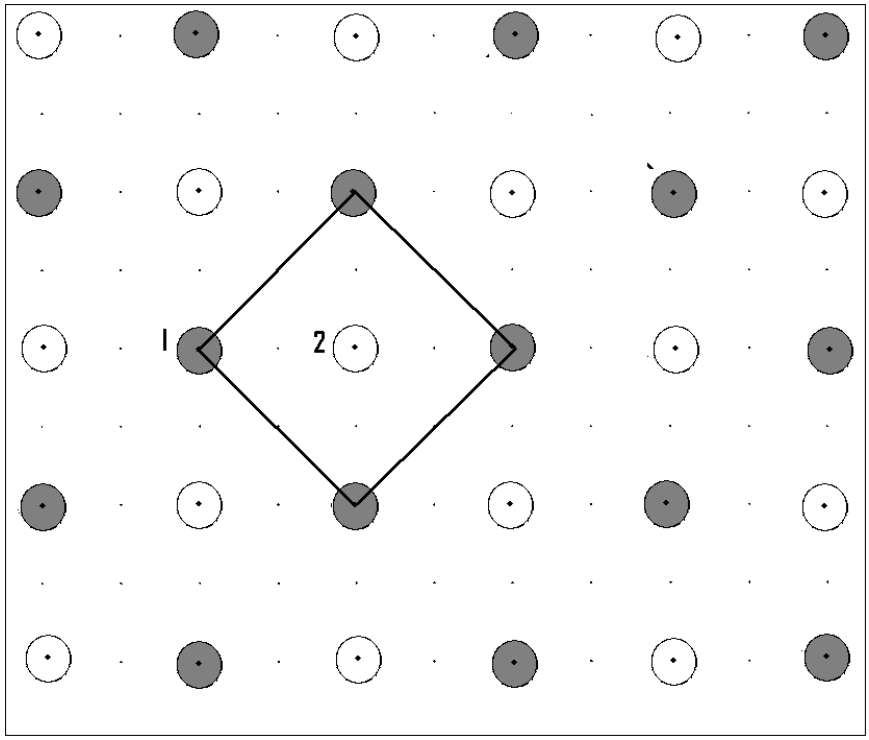

Figure 5. The rock salt structure after the 4-atom unit cell transition.

Figures 6 and 7 show how the planes would slide in this mechanism. Instead of all the plane pairs sliding the same direction relative to the ones before it, each pair slides in the direction opposite to the one before. The advantage to this mechanism is that it requires a much lower deformation in the crystal as a whole, helping it to have the lowest barrier height of all the ones we calculated.

Encouraged by the fact that the transition mechanisms with no broken bonds are also the most favorable for SiC, we did a run for COMSUBS that included larger cell sizes. The larger cell sizes take several times longer to do energy calculations, so we only did calculations for the mechanisms that do not break any bonds. We found that their enthalpies are only slightly higher than the most favorable mechanism we found in the

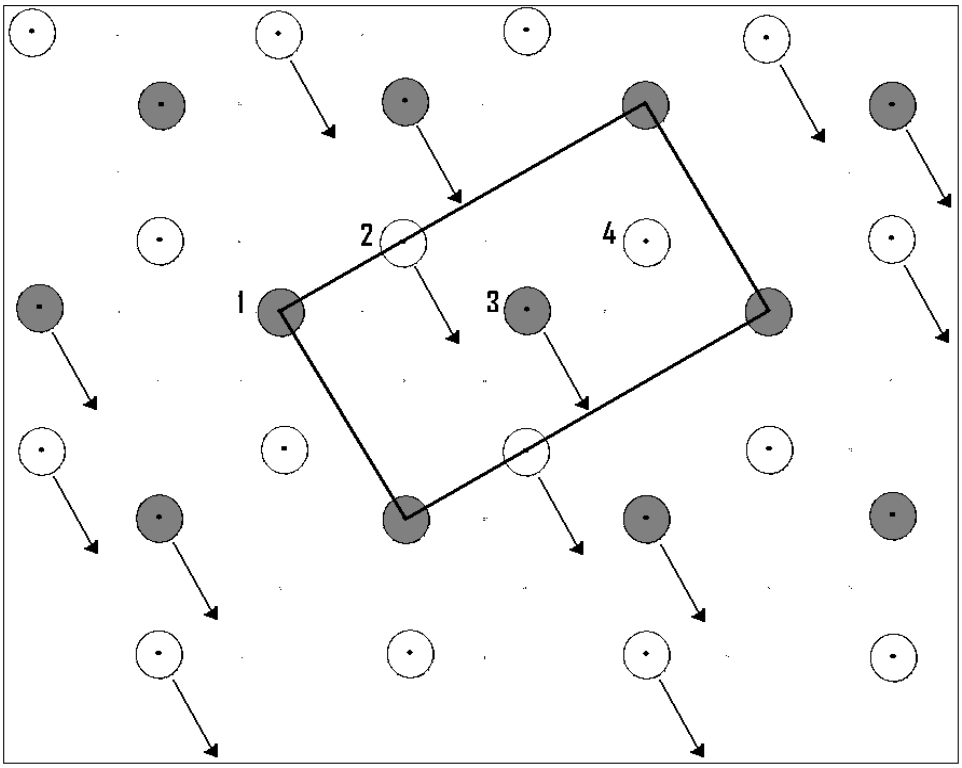

Figure 6. Transition mechanism with 8 atoms, 4 atom pairs, in the unit cell. Each pair of planes slides in alternating directions relative to the prior one.

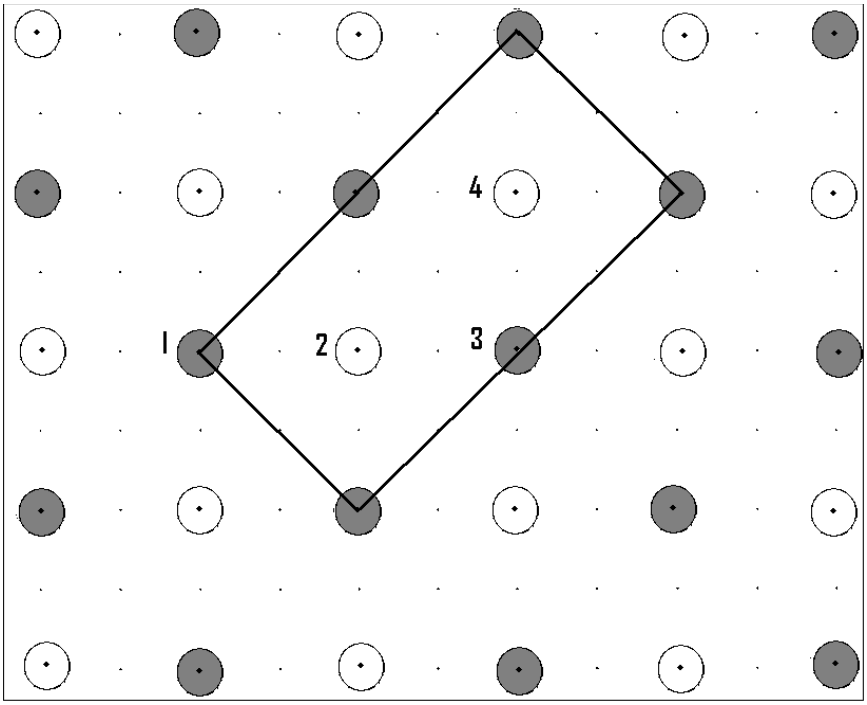

Figure 7. The rock salt structure after the 8-atom unit cell transition.

smaller run and significantly lower than the other mechanisms we studied, including the mechanism that is the second most favorable of the smaller run.

The no bond breaking mechanism of the larger run that had 12 atoms per unit cell, listed as Subgroup 3 in Appendix B, is shown in Figures 8 and 9. The sliding mechanism repeats for every third pair of planes. This is the final mechanism found by Shimojo which he labeled RS-III. We also found two 16-atom and three 20-atom mechanisms that had no broken bonds, listed as Subgroups 4-8 in Appendix B. These mechanisms were not mentioned anywhere else in the literature that we searched. After we found the general mechanism for the phase transition, we were able to predict the existence of all of the 20 atoms per unit cell mechanisms before we did a COMSUBS run large enough to find them.

Limpijumnong and Lambrecht (2001) proposed that the 4-atom pathway passes through an intermediate structure with tetragonal symmetry. We optimized this tetragonal structure at 60 GPa using FIREBALL and found its enthalpy to be greater than any point along the pathway.

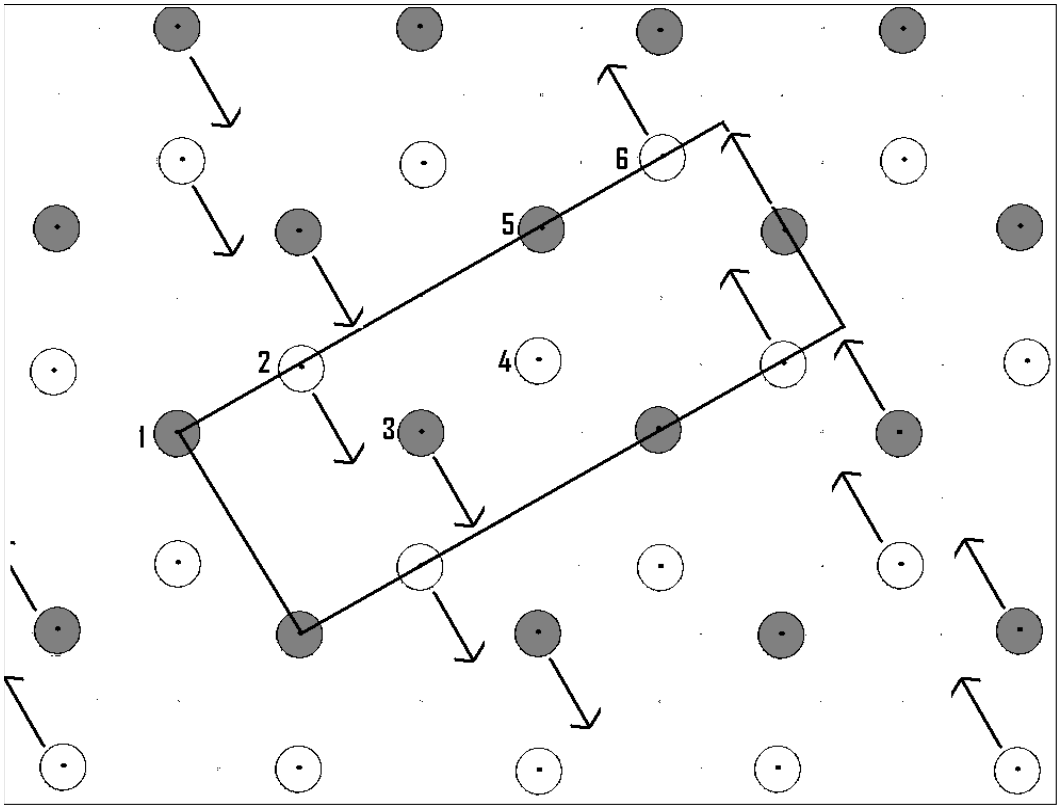

Figure 8. Transition mechanism with 12 atoms, 6 atom pairs, in the unit cell. Each pair of planes slides in a pattern that repeats every third pair.

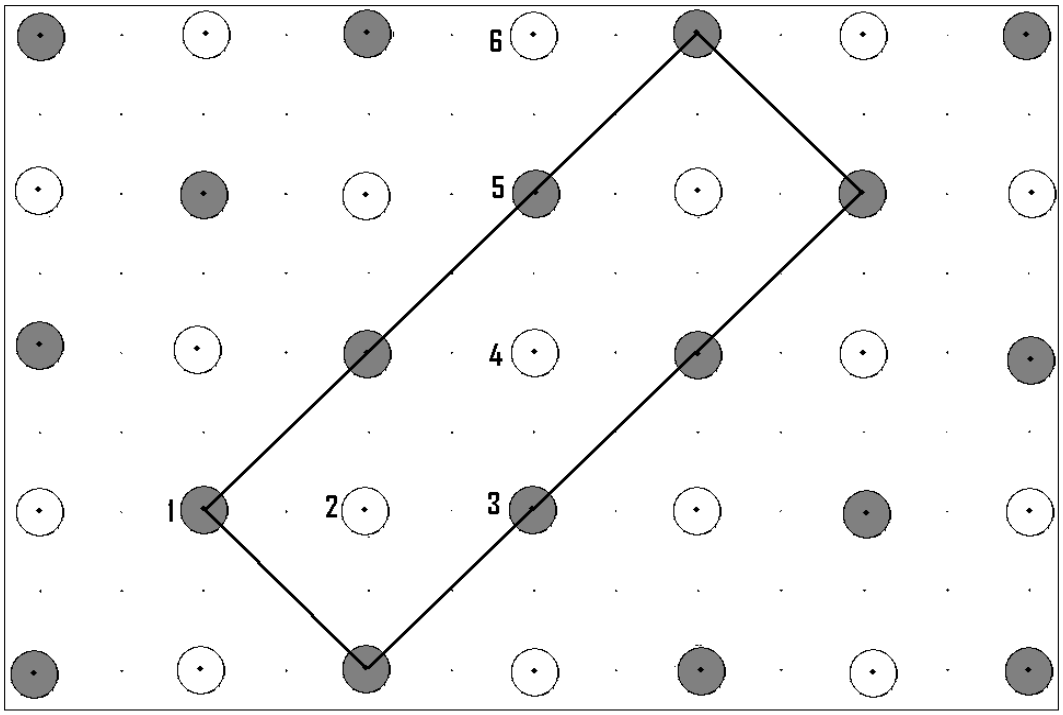

Figure 9. The rock salt structure after the 12-atom unit cell transition.

III Conclusions

With COMSUBS and FIREBALL we were able to find and evaluate a far larger number of possible mechanisms for GaN's phase transitions than would have been possible otherwise. COMSUBS easily found all the mechanisms in the literature for the wurtzite to rock salt transition. With FIREBALL we were able to verify that those mechanisms are among the most favorable for GaN. While Shimojo found the same mechanisms we did for the smaller unit cell sizes, he failed to understand the general mechanism of the wurtzite to rock salt phase transition. In the other papers we read, they only proposed the simplest mechanism, our Subgroup 1 in Appendix B.

We were able to find the general mechanism that included all of the mechanisms that we found that had zero broken bonds. All of these mechanisms involve the sliding of pairs of (010) planes about half the lattice parameter length *a* in the positive or negative [100] direction relative to the adjacent pairs of planes. Table I represents all the mechanisms that we have listed in Appendix B. A plus (+) represents the plane pairs sliding one half of the unit vector in the positive [100] direction relative to the prior pair while a minus (-) represents a slide in the negative [100] direction. The pattern for each mechanism is repeated throughout the crystal (see Figures 4, 6 and 8).

Once we found a general mechanism using our first three no-bond-breaking mechanisms, we were able to create more possible mechanisms by inspection and verify them by expanding of the search of COMSUBS to larger cell sizes. Now that the general mechanism is verified we can write down by inspection possible transition mechanisms for any cell size.

Table I. Pattern of mechanisms that had no bonds broken.

Atoms in each unit cell	*Direction of plane sliding*	*Barrier Height*
4	+	0.101 eV/atom
8	+ -	0.071
12	+ + -	0.077
16	+ + - -	0.087
16	+ + + -	
20	+ + + + -	
20	+ + + - -	
20	+ + - + -	

The methods that we used to find the phase transition mechanisms for SiC and GaN can now be applied to other materials. Our methods allow us to make a faster and more complete search of possible mechanisms. Given a large enough number of favorable mechanisms, a general mechanism can then be found. We have seen from the materials that we have already studied that favorable mechanisms are likely to have no bonds broken during the transition and are likely to involve the sliding of parallel planes of atoms.

Appendix A

Structural Parameters of Select Space Groups

Spacegroup 225
Basis Vectors
(0,1/2,1/2),(1/2,0,1/2),(1/2,1/2,0)
Wyckoff Points Coordinates

a	(0,0,0)
b	(1/2,1/2,1/2)
c	(1/4,1/4,1/4), (-1/4,-1/4,-1/4)
d	(0,1/4,1/4), (0,1/4,-1/4), (1/4,1/4,0), (1/4,-1/4,0), (1/4,0,1/4), (1/4,0,-1/4)
e	(x,0,0), (-x,0,0), (0,0,x), (0,0,-x), (0,x,0), (0,-x,0)
f	(x,x,x), (x,-x,-x), (-x,x,-x), (-x,-x,x), (-x,-x,-x), (-x,x,x), (x,-x,x), (x,x,-x)
g	(x,1/4,1/4), (-x,1/4,-1/4), (1/4,1/4,x), (1/4,-1/4,-x), (1/4,x,1/4), (1/4,-x,-1/4), (-1/4,-x,-1/4), (-1/4,x,1/4), (-x,-1/4,-1/4), (x,-1/4,1/4), (-1/4,-1/4,-x), (-1/4,1/4,x)

Spacegroup 186
Basis Vectors
(1,0,0),(0,1,0),(0,0,1)
Wyckoff Points Coordinates

a	(0,0,z), (0,0,z+1/2)
b	(1/3,2/3,z), (-1/3,1/3,z+1/2)
c	(x,-x,z), (2x,x,z+1/2), (x,2x,z), (-x,x,z+1/2), (-2x,-x,z), (-x,-2x,z+1/2)
d	(x,y,z), (x-y,x,z+1/2), (-y,x-y,z), (-x,-y,z+1/2), (-x+y,-x,z), (y,-x+y,z+1/2), (-x+y,y,z), (-x,-x+y,z+1/2), (-y,-x,z), (x-y,-y,z+1/2), (x,x-y,z), (y,x,z+1/2)

Spacegroup 36
Basis Vectors

(1/2,-1/2,0),(1/2,1/2,0),(0,0,1)
Wyckoff Points Coordinates
a (0,y,z), (0,-y,z+1/2)
b (x,y,z), (-x,-y,z+1/2),
(-x,y,z), (x,-y,z+1/2)

Spacegroup 33
Basis Vectors
(1,0,0),(0,1,0),(0,0,1)
Wyckoff Points Coordinates
a (x,y,z), (-x,-y,z+1/2),
(-x+1/2,y+1/2,z+1/2), (x+1/2,-y+1/2,z)

Spacegroup 8
Basis Vectors
(0,0,1),(1/2,1/2,0),(-1/2,1/2,0)
Wyckoff Points Coordinates
a (x,0,z)
b (x,y,z), (x,-y,z)

Spacegroup 4
Basis Vectors
(0,0,1),(1,0,0),(0,1,0)
Wyckoff Points Coordinates
a (x,y,z), (-x,y+1/2,-z)

Spacegroup 1
Basis Vectors
(0,0,1),(1,0,0),(0,1,0)
Wyckoff Points Coordinates
a (x,y,z)

Appendix B

Zero Bond Breaking Transition Mechanisms

```
comsubs, version 2.2, April 2005
Harold T. Stokes and Dorian M. Hatch, Brigham Young University
Mon May  9 14:04:47 2005

GaN
First crystal:
  Space group: 186 P6_3mc
  Lattice parameters:    3.0800 3.0800 5.0600  90.0000  90.0000 120.0000
  Number of Wyckoff positions:   2
  N, Wyckoff position b,    0.33333   0.66667   0.00000
  Ga, Wyckoff position b,    0.33333   0.66667   0.37400
Second crystal:
  Space group: 225 Fm-3m
  Lattice parameters:    4.1900 4.1900 4.1900  90.0000  90.0000  90.0000
  Number of Wyckoff positions:   2
  N, Wyckoff position a,    0.00000   0.00000   0.00000
  Ga, Wyckoff position b,    0.50000   0.50000   0.50000
Minimum size of unit cell:   1
Maximum size of unit cell:   5
Minimum strain: .600
Maximum strain: 1.60
Minimum distance between atoms:    1.500
Constrain shuffle to  2.00
Conserve bonds of length less than       2.20
Number of atoms in primitive unit cell of crystal 1:   4
Number of atoms in primitive unit cell of crystal 2:   2
Volume/atom in crystal 1:     10.393
Volume/atom in crystal 2:      9.195
Nearest distance between atoms in crystal 1:    1.8891
Nearest distance between atoms in crystal 2:    2.0950
---------------------------------------
Subgroup     1
Principal values of strain tensor:    1.360   0.828   0.785
Nearest-neighbor distance along path:    1.868
Broken bonds:  0 out of  8
Maximum atomic shuffle:    0.547
Common subgroup:  36 Cmc2_1
Setting of crystal 1:
  Size =  1
  Lattice: (1,1,0),(-1,1,0),(0,0,1)
  Origin: (0,0,0)
```

```
  Lattice parameters:    3.0800 5.3347 5.0600  90.0000  90.0000  90.0000
  N  a  y'=-0.33333, z'= 0.00000
  Ga a  y'=-0.33333, z'= 0.37400
Setting of crystal 2:
  Size =  2
  Lattice: (0,-1,0),(0,0,-1),(1,0,0)
  Origin: (3/50,1/2,1/4)
  Lattice parameters:    4.1900 4.1900 4.1900  90.0000  90.0000  90.0000
  N  a  y'=-0.25000, z'=-0.06300
  Ga a  y'=-0.25000, z'= 0.43700
At midpoint:
  Lattice parameters:    3.6089 4.7281 4.5918  90.0000  90.0000  90.0000
  N  a  y'=-0.29167, z'=-0.03150
  Ga a  y'=-0.29167, z'= 0.40550
---------------------------------------
Subgroup     2
Principal values of strain tensor:    1.111   0.962   0.828
Nearest-neighbor distance along path:    1.801
Broken bonds:  0 out of 16
Maximum atomic shuffle:    0.863
Common subgroup:  33 Pna2_1
Setting of crystal 1:
  Size =  2
  Lattice: (1,2,0),(-1,0,0),(0,0,1)
  Origin: (0,0,0)
  Lattice parameters:    5.3347 3.0800 5.0600  90.0000  90.0000  90.0000
  N  a  x'= 0.33333, y'= 0.00000, z'= 0.00000
  Ga a  x'= 0.33333, y'= 0.00000, z'= 0.37400
Setting of crystal 2:
  Size =  4
  Lattice: (0,1,-1),(0,1/2,1/2),(1,0,0)
  Origin: (3/50,-1/4,1/2)
  Lattice parameters:    5.9256 2.9628 4.1900  90.0000  90.0000  90.0000
  N  a  x'= 0.37500, y'=-0.25000, z'=-0.06300
  Ga a  x'= 0.37500, y'=-0.25000, z'= 0.43700
At midpoint:
  Lattice parameters:    5.6224 3.0172 4.6186  90.0000  90.0000  90.0000
  N  a  x'= 0.35417, y'=-0.12500, z'=-0.03150
  Ga a  x'= 0.35417, y'=-0.12500, z'= 0.40550
---------------------------------------
Subgroup     3
Principal values of strain tensor:    1.159   0.922   0.828
Nearest-neighbor distance along path:    1.770
Broken bonds:  0 out of 24
Maximum atomic shuffle:    1.219
```

Common subgroup: 4 P2_1
Setting of crystal 1:
 Size = 3
 Lattice: (-1,0,0),(0,0,1),(0,3,0)
 Origin: (0,1,0)
 Lattice parameters: 3.0800 5.0600 9.2400 90.0000 60.0000 90.0000
 N a x'= 0.66667, y'= 0.00000, z'= 0.88889
 N a x'= 0.33333, y'= 0.50000, z'= 0.77778
 N a x'= 0.66667, y'= 0.00000, z'= 0.55556
 Ga a x'= 0.66667, y'= 0.37400, z'= 0.88889
 Ga a x'= 0.33333, y'= 0.87400, z'= 0.77778
 Ga a x'= 0.66667, y'= 0.37400, z'= 0.55556
Setting of crystal 2:
 Size = 6
 Lattice: (0,1/2,1/2),(1,0,0),(0,2,-1)
 Origin: (3/50,1/2,1/4)
 Lattice parameters: 2.9628 4.1900 9.3691 90.0000 71.5651 90.0000
 N a x'= 0.33333, y'=-0.06300, z'= 0.91667
 N a x'= 0.00000, y'= 0.43700, z'= 0.75000
 N a x'= 0.66667, y'=-0.06300, z'= 0.58333
 Ga a x'= 0.33333, y'= 0.43700, z'= 0.91667
 Ga a x'= 0.00000, y'= 0.93700, z'= 0.75000
 Ga a x'= 0.66667, y'= 0.43700, z'= 0.58333
At midpoint:
 Lattice parameters: 3.0124 4.6113 9.2769 90.0000 65.7825 90.0000
 N a x'= 0.50000, y'=-0.03150, z'= 0.90278
 N a x'= 0.16667, y'= 0.46850, z'= 0.76389
 N a x'= 0.66667, y'=-0.03150, z'= 0.56944
 Ga a x'= 0.50000, y'= 0.40550, z'= 0.90278
 Ga a x'= 0.16667, y'= 0.90550, z'= 0.76389
 Ga a x'= 0.66667, y'= 0.40550, z'= 0.56944

Subgroup 4
Principal values of strain tensor: 1.111 0.962 0.828
Nearest-neighbor distance along path: 1.801
Broken bonds: 0 out of 32
Maximum atomic shuffle: 1.588
Common subgroup: 33 Pna2_1
Setting of crystal 1:
 Size = 4
 Lattice: (2,4,0),(-1,0,0),(0,0,1)
 Origin: (1/2,3/2,0)
 Lattice parameters: 10.6694 3.0800 5.0600 90.0000 90.0000 90.0000
 N a x'= 0.79167, y'= 0.75000, z'= 0.00000
 N a x'= 0.04167, y'= 0.25000, z'= 0.00000

Ga a x'= 0.79167, y'= 0.75000, z'= 0.37400
Ga a x'= 0.04167, y'= 0.25000, z'= 0.37400
Setting of crystal 2:
Size = 8
Lattice: (0,2,-2),(0,1/2,1/2),(1,0,0)
Origin: (3/50,3/4,0)
Lattice parameters: 11.8511 2.9628 4.1900 90.0000 90.0000 90.0000
N a x'= 0.81250, y'= 0.25000, z'=-0.06300
N a x'= 0.06250, y'= 0.25000, z'=-0.06300
Ga a x'= 0.81250, y'= 0.25000, z'= 0.43700
Ga a x'= 0.06250, y'= 0.25000, z'= 0.43700
At midpoint:
Lattice parameters: 11.2448 3.0172 4.6186 90.0000 90.0000 90.0000
N a x'= 0.80208, y'= 0.50000, z'=-0.03150
N a x'= 0.05208, y'= 0.25000, z'=-0.03150
Ga a x'= 0.80208, y'= 0.50000, z'= 0.40550
Ga a x'= 0.05208, y'= 0.25000, z'= 0.40550

Subgroup 5
Principal values of strain tensor: 1.203 0.888 0.828
Nearest-neighbor distance along path: 1.752
Broken bonds: 0 out of 32
Maximum atomic shuffle: 1.402
Common subgroup: 4 P2_1
Setting of crystal 1:
Size = 4
Lattice: (-1,0,0),(0,0,1),(0,4,0)
Origin: (0,1,0)
Lattice parameters: 3.0800 5.0600 12.3200 90.0000 60.0000 90.0000
N a x'= 0.66667, y'= 0.00000, z'= 0.91667
N a x'= 0.33333, y'= 0.50000, z'= 0.83333
N a x'= 0.66667, y'= 0.00000, z'= 0.41667
N a x'= 0.33333, y'= 0.50000, z'= 0.33333
Ga a x'= 0.66667, y'= 0.37400, z'= 0.91667
Ga a x'= 0.33333, y'= 0.87400, z'= 0.83333
Ga a x'= 0.66667, y'= 0.37400, z'= 0.41667
Ga a x'= 0.33333, y'= 0.87400, z'= 0.33333
Setting of crystal 2:
Size = 8
Lattice: (0,1/2,1/2),(1,0,0),(0,5/2,-3/2)
Origin: (3/50,1/2,1/4)
Lattice parameters: 2.9628 4.1900 12.2158 90.0000 75.9638 90.0000
N a x'= 0.31250, y'=-0.06300, z'= 0.93750
N a x'=-0.06250, y'= 0.43700, z'= 0.81250
N a x'= 0.81250, y'=-0.06300, z'= 0.43750

```
  N  a  x'= 0.43750, y'= 0.43700, z'= 0.31250
  Ga a  x'= 0.31250, y'= 0.43700, z'= 0.93750
  Ga a  x'=-0.06250, y'= 0.93700, z'= 0.81250
  Ga a  x'= 0.81250, y'= 0.43700, z'= 0.43750
  Ga a  x'= 0.43750, y'= 0.93700, z'= 0.31250
At midpoint:
  Lattice parameters:   3.0072 4.6033 12.2103  90.0000  67.9819  90.0000
  N  a  x'= 0.48958, y'=-0.03150, z'= 0.92708
  N  a  x'= 0.13542, y'= 0.46850, z'= 0.82292
  N  a  x'= 0.73958, y'=-0.03150, z'= 0.42708
  N  a  x'= 0.38542, y'= 0.46850, z'= 0.32292
  Ga a  x'= 0.48958, y'= 0.40550, z'= 0.92708
  Ga a  x'= 0.13542, y'= 0.90550, z'= 0.82292
  Ga a  x'= 0.73958, y'= 0.40550, z'= 0.42708
  Ga a  x'= 0.38542, y'= 0.90550, z'= 0.32292
---------------------------------------
Subgroup     6
Principal values of strain tensor:    1.131    0.945    0.828
Nearest-neighbor distance along path:    1.783
Broken bonds:  0 out of 40
Maximum atomic shuffle:    1.964
Common subgroup:   4 P2_1
Setting of crystal 1:
  Size =  5
  Lattice: (-1,0,0),(0,0,1),(0,5,0)
  Origin: (0,3/2,0)
  Lattice parameters:   3.0800 5.0600 15.4000  90.0000  60.0000  90.0000
  N  a  x'= 0.66667, y'= 0.00000, z'= 0.83333
  N  a  x'= 0.33333, y'= 0.50000, z'= 0.76667
  N  a  x'= 0.66667, y'= 0.00000, z'= 0.03333
  N  a  x'= 0.66667, y'= 0.00000, z'= 0.43333
  N  a  x'= 0.33333, y'= 0.50000, z'= 0.36667
  Ga a  x'= 0.66667, y'= 0.37400, z'= 0.83333
  Ga a  x'= 0.33333, y'= 0.87400, z'= 0.76667
  Ga a  x'= 0.66667, y'= 0.37400, z'= 0.03333
  Ga a  x'= 0.66667, y'= 0.37400, z'= 0.43333
  Ga a  x'= 0.33333, y'= 0.87400, z'= 0.36667
Setting of crystal 2:
  Size = 10
  Lattice: (0,1/2,1/2),(1,0,0),(0,7/2,-3/2)
  Origin: (3/50,1,1/4)
  Lattice parameters:   2.9628 4.1900 15.9550  90.0000  68.1986  90.0000
  N  a  x'= 0.05000, y'=-0.06300, z'= 0.85000
  N  a  x'=-0.25000, y'= 0.43700, z'= 0.75000
  N  a  x'= 0.65000, y'=-0.06300, z'= 0.05000
```

N a x'= 0.85000, y'=-0.06300, z'= 0.45000
N a x'= 0.55000, y'= 0.43700, z'= 0.35000
Ga a x'= 0.05000, y'= 0.43700, z'= 0.85000
Ga a x'=-0.25000, y'= 0.93700, z'= 0.75000
Ga a x'= 0.65000, y'= 0.43700, z'= 0.05000
Ga a x'= 0.85000, y'= 0.43700, z'= 0.45000
Ga a x'= 0.55000, y'= 0.93700, z'= 0.35000
At midpoint:
Lattice parameters: 3.0153 4.6156 15.6458 90.0000 64.0993 90.0000
N a x'= 0.35833, y'=-0.03150, z'= 0.84167
N a x'= 0.04167, y'= 0.46850, z'= 0.75833
N a x'= 0.65833, y'=-0.03150, z'= 0.04167
N a x'= 0.75833, y'=-0.03150, z'= 0.44167
N a x'= 0.44167, y'= 0.46850, z'= 0.35833
Ga a x'= 0.35833, y'= 0.40550, z'= 0.84167
Ga a x'= 0.04167, y'= 0.90550, z'= 0.75833
Ga a x'= 0.65833, y'= 0.40550, z'= 0.04167
Ga a x'= 0.75833, y'= 0.40550, z'= 0.44167
Ga a x'= 0.44167, y'= 0.90550, z'= 0.35833

Subgroup 7
Principal values of strain tensor: 1.131 0.945 0.828
Nearest-neighbor distance along path: 1.783
Broken bonds: 0 out of 40
Maximum atomic shuffle: 1.365
Common subgroup: 4 P2_1
Setting of crystal 1:
Size = 5
Lattice: (-1,0,0),(0,0,1),(0,5,0)
Origin: (0,2,0)
Lattice parameters: 3.0800 5.0600 15.4000 90.0000 60.0000 90.0000
N a x'= 0.66667, y'= 0.00000, z'= 0.73333
N a x'= 0.33333, y'= 0.50000, z'= 0.66667
N a x'= 0.66667, y'= 0.00000, z'= 0.93333
N a x'= 0.33333, y'= 0.50000, z'= 0.86667
N a x'= 0.66667, y'= 0.00000, z'= 0.53333
Ga a x'= 0.66667, y'= 0.37400, z'= 0.73333
Ga a x'= 0.33333, y'= 0.87400, z'= 0.66667
Ga a x'= 0.66667, y'= 0.37400, z'= 0.93333
Ga a x'= 0.33333, y'= 0.87400, z'= 0.86667
Ga a x'= 0.66667, y'= 0.37400, z'= 0.53333
Setting of crystal 2:
Size = 10
Lattice: (0,1/2,1/2),(1,0,0),(0,7/2,-3/2)
Origin: (3/50,5/4,0)

Lattice parameters: 2.9628 4.1900 15.9550 90.0000 68.1986 90.0000
N a x'= 0.25000, y'=-0.06300, z'= 0.75000
N a x'=-0.05000, y'= 0.43700, z'= 0.65000
N a x'= 0.85000, y'=-0.06300, z'= 0.95000
N a x'= 0.55000, y'= 0.43700, z'= 0.85000
N a x'= 0.65000, y'=-0.06300, z'= 0.55000
Ga a x'= 0.25000, y'= 0.43700, z'= 0.75000
Ga a x'=-0.05000, y'= 0.93700, z'= 0.65000
Ga a x'= 0.85000, y'= 0.43700, z'= 0.95000
Ga a x'= 0.55000, y'= 0.93700, z'= 0.85000
Ga a x'= 0.65000, y'= 0.43700, z'= 0.55000
At midpoint:
Lattice parameters: 3.0153 4.6156 15.6458 90.0000 64.0993 90.0000
N a x'= 0.45833, y'=-0.03150, z'= 0.74167
N a x'= 0.14167, y'= 0.46850, z'= 0.65833
N a x'= 0.75833, y'=-0.03150, z'= 0.94167
N a x'= 0.44167, y'= 0.46850, z'= 0.85833
N a x'= 0.65833, y'=-0.03150, z'= 0.54167
Ga a x'= 0.45833, y'= 0.40550, z'= 0.74167
Ga a x'= 0.14167, y'= 0.90550, z'= 0.65833
Ga a x'= 0.75833, y'= 0.40550, z'= 0.94167
Ga a x'= 0.44167, y'= 0.90550, z'= 0.85833
Ga a x'= 0.65833, y'= 0.40550, z'= 0.54167

Subgroup 8
Principal values of strain tensor: 1.232 0.867 0.828
Nearest-neighbor distance along path: 1.742
Broken bonds: 0 out of 40
Maximum atomic shuffle: 1.514
Common subgroup: 4 P2_1
Setting of crystal 1:
Size = 5
Lattice: (-1,0,0),(0,0,1),(0,5,0)
Origin: (0,1,0)
Lattice parameters: 3.0800 5.0600 15.4000 90.0000 60.0000 90.0000
N a x'= 0.66667, y'= 0.00000, z'= 0.93333
N a x'= 0.33333, y'= 0.50000, z'= 0.86667
N a x'= 0.66667, y'= 0.00000, z'= 0.33333
N a x'= 0.33333, y'= 0.50000, z'= 0.26667
N a x'= 0.66667, y'= 0.00000, z'= 0.53333
Ga a x'= 0.66667, y'= 0.37400, z'= 0.93333
Ga a x'= 0.33333, y'= 0.87400, z'= 0.86667
Ga a x'= 0.66667, y'= 0.37400, z'= 0.33333
Ga a x'= 0.33333, y'= 0.87400, z'= 0.26667
Ga a x'= 0.66667, y'= 0.37400, z'= 0.53333

Setting of crystal 2:
  Size = 10
  Lattice: (0,1/2,1/2),(1,0,0),(0,3,-2)
  Origin: (3/50,1/2,1/4)
  Lattice parameters: 2.9628 4.1900 15.1073 90.0000 78.6901 90.0000
  N a x'= 0.30000, y'=-0.06300, z'= 0.95000
  N a x'=-0.10000, y'= 0.43700, z'= 0.85000
  N a x'= 0.90000, y'=-0.06300, z'= 0.35000
  N a x'= 0.50000, y'= 0.43700, z'= 0.25000
  N a x'= 0.70000, y'=-0.06300, z'= 0.55000
  Ga a x'= 0.30000, y'= 0.43700, z'= 0.95000
  Ga a x'=-0.10000, y'= 0.93700, z'= 0.85000
  Ga a x'= 0.90000, y'= 0.43700, z'= 0.35000
  Ga a x'= 0.50000, y'= 0.93700, z'= 0.25000
  Ga a x'= 0.70000, y'= 0.43700, z'= 0.55000
At midpoint:
  Lattice parameters: 3.0032 4.5972 15.1619 90.0000 69.3450 90.0000
  N a x'= 0.48333, y'=-0.03150, z'= 0.94167
  N a x'= 0.11667, y'= 0.46850, z'= 0.85833
  N a x'= 0.78333, y'=-0.03150, z'= 0.34167
  N a x'= 0.41667, y'= 0.46850, z'= 0.25833
  N a x'= 0.68333, y'=-0.03150, z'= 0.54167
  Ga a x'= 0.48333, y'= 0.40550, z'= 0.94167
  Ga a x'= 0.11667, y'= 0.90550, z'= 0.85833
  Ga a x'= 0.78333, y'= 0.40550, z'= 0.34167
  Ga a x'= 0.41667, y'= 0.90550, z'= 0.25833
  Ga a x'= 0.68333, y'= 0.40550, z'= 0.54167
---
done

References

D. M. Hatch, H. T. Stokes, J. Dong, J. Gunter, H. Wang, and J. P. Lewis, "Bilayer sliding mechanism for the zinc-blende to rock salt transition in SiC," Phys. Rev. B **71**, 184109 (2005).

J. P. Lewis, K. R. Glaesemann, G. A. Voth, J. Fritsch, A. A. Demkov, J. Ortega, O. F. Sankey, "Further developments in the local-orbital density-functional-theory tight-binding method," Phys. Rev. B **64**, 195103 (2001).

S. Limpijumnong and W. R. L. Lambrecht, "Homogeneous strain deformation path for the wurtzite to rock salt high-pressure phase transition in GaN," Phys. Rev. Letters **86**, 91 (2001).

A. M. Saitta and F. Decremps, "Unifying description of the wurtzite-to-rock salt phase transition in wide-gap semiconductors: The effect of d electrons on the elastic constants", Phys. Rev. B **70**, 035214 (2004).

F. Shimojo, S. Kodiyalam, I. Ebbsjo, R. K. Kalia, A. Nakano, and P. Vashishta, "Atomistic mechanisms for wurtzite-to-rock salt structural transformation in cadmium selenide under pressure", Phys. Rev. B **70**, 184111 (2004).

H. Sowa, "On the transition from the wurtzite to the NaCl type", Acta Cryst. **A57**, 176 (2001).

H. T. Stokes and D.M. Hatch, Isotropy Software Package, http://stokes.byu.edu/isotropy.html, (2004).

H. Xia, Q. Xia, and A. L. Ruoff, "High-pressure structure of gallium nitride wurtizite to rock salt phase transition," Phys. Rev. B **47,** 12925 (1993).